Nanoscale

PAPER

View Article Online
View Journal | View Issue

Cite this: *Nanoscale*, 2016, **8**, 12998

Osmotic pressure-dependent release profiles of payloads from nanocontainers by co-encapsulation of simple salts†

Shahed Behzadi, Christine Rosenauer, Michael Kappl, Kristin Mohr, Katharina Landfester and Daniel Crespy*

Received 4th March 2016,
Accepted 27th May 2016

DOI: 10.1039/c6nr01882c

www.rsc.org/nanoscale

The encapsulation of payloads in micro- to nano-scale capsules allows protection of the payload from the surrounding environment and control of its release profile. Herein, we program the release of hydrophilic payloads from nanocontainers by co-encapsulating simple inorganic salts for adjusting the osmotic pressure. The latter either leads to a burst release at high concentrations of co-encapsulated salts or a sustained release at lower concentrations. Osmotic pressure causes swelling of the nanocapsule's shell and therefore sustained release profiles can be adjusted by crosslinking it. The approach presented allows for programing the release of payloads by co-encapsulating inexpensive salts inside nanocontainers without the help of stimuli-responsive materials.

Introduction

Osmotic pressure is a crucial phenomenon in nature.[1,2] The cell maintains the concentration of solutes *via* osmotic pressure[1] and plants rely on it to absorb water and maintain cell rigidity.[2] The control of osmotic pressure is important for medical care and water purification to avoid breakdown of the cell membrane (lysis), for storage of red blood cells,[3] for dialysis in artificial kidneys,[4] to control osmotic dehydration in food preservation,[5] and to apply reverse osmosis for water desalination.[6] In recent decades, miniaturized devices consisting of a thin membrane have found applications in many areas of science and technology.[7–9]

Micro- to nano-scale polymer capsules – which are defined as a liquid core surrounded by a polymer membrane – are well-known controlled release systems. The use of these capsules for medical and technical purposes has rapidly been expanding.[10–13] Regardless of the application, controlled release of the payload is the dominating function of capsules. The term "controlled release" includes a range of different release profiles and mechanisms such as targeted release,[14] triggered release,[15] and sustained (or extended) release.[16] Modification of the membrane's physicochemical properties is of utmost importance to achieve a desired release profile.[17–19] Considerable efforts have been devoted to achieve these types of release profiles by modifying the physicochemical properties of the membrane. These efforts include the use of novel stimuli-responsive functional groups.[20–22] In the case of sustained release, the desired lifetime of release highly depends on the targeted applications. As an example, the desired life-time of release for pharmaceutical applications is roughly one day whereas for coatings it can be thousands of days.[12,23]

However, to avoid synthetic complexity, there is huge interest in simple strategies for the release of the payload in a controlled fashion. The overall release of the payload is explained as a sum of two contributions – these are burst and (slow) diffusive release.[24] Osmotic pressure can be used as a trigger for burst release profiles.[25] For drug delivery systems, burst release profiles were achieved *via* osmotic pressure for various types of macroscopic ($D \sim 6$ mm) capsules with an asymmetric membrane.[26,27] As another example, the release properties of microcapsules were controlled by osmotic pressure generated by either the dissolution of the encapsulated materials[28–31] or the addition of an osmotic agent in the release media.[32–34] It is believed that osmotic pressure imposes stress on the membrane of microcapsules that largely accelerate the release of payloads once the membrane bursts.[28,31–33,35,36] However, membrane rupture arising from osmotic pressure is detrimental for some applications. Indeed, the initial high release rate may lead to drug concentrations near or above the toxic level *in vivo*.[25,37] Preventing a burst profile is therefore crucial, especially with low molecular weight payloads (*e.g.* drugs) which are more likely to display a burst release due to high osmotic pressure and their small size.[38–40] Crosslinking[41,42] and increasing of the shell thickness[43,44] are expected to have

Max Planck Institute for Polymer Research, D-55128 Mainz, Germany.
E-mail: crespy@mpip-mainz.mpg.de

†Electronic supplementary information (ESI) available. See DOI: 10.1039/c6nr01882c

an influence on the shell permeation and subsequently suppress the release of the payloads from the nanocapsules (NCs) despite an osmotic pressure difference. A major problem in osmotically driven release systems is the lack of control over the ratio of burst and diffusive contributions. The control over these properties plays a key role for advanced applications. A very simple model predicts that the burst release is proportional to osmotic pressure and the quadratic functions of size and membrane thickness.[45–47]

The deformation of capsules by osmotic pressure can be measured and predicted. This feature allowed Kim *et al*. to use microcapsules prepared *via* microfluidics to calculate the osmotic strength of solutions by measuring the buckling of these microcapsules.[48] Since nanocapsules, as their name suggests, are very small and have a thin membrane, their release profile can be tuned more effectively by controlling the osmotic pressure. However, how the release profiles can be tuned as a function of osmotic pressure remains unclear.

We aim at programming the release profile of nanocapsules from burst release to sustained release by using the osmotic pressure as a trigger and without the use of other stimuli-responsive materials. To fulfill this goal, we prepared NCs containing a dye and low to high concentrations of potassium chloride (KCl) or calcium chloride ($CaCl_2$). These two salts were chosen since they are easily available and inexpensive. Firstly, we quantified the influence of co-encapsulated salts on the release profile of a dye at different salt concentrations. The release experiments were carried out at room temperature (22–25 °C). A detailed insight into the correlation between the released fraction of the dye and the co-encapsulated salts was obtained.

Results and discussion

Preparation of polyurea NCs

Aliphatic–aromatic polyurea has a number of interesting advantages including fairly good mechanical performance and high chemical resistance.[49–51] Furthermore, polyurea can be prepared by a wide range of monomers/polymers and chemical reactions for the preparation of the polymer shell.[52] The formation of polyurea shells was performed through a polyaddition reaction between the primary amino groups ($-NH_2$) of hydrophilic 1,4-diaminobutane and the isocyanate group (–NCO) of 2,4-toluene diisocyanate (TDI) that occurs at the interface of miniemulsion droplets.[52] Polyurea NCs with an average hydrodynamic diameter of 318 ± 98 nm containing the payloads were obtained (see Fig. 1a and Table S1†). After the synthesis, the obtained polyurea NCs were transferred in an aqueous solution of sodium dodecyl sulfate (SDS) (0.3 wt%). The critical micelle concentration (CMC) of SDS is reported to be 2.38 g L^{-1} at 25 °C in water.[53] Although the SDS concentration in the aqueous dispersion is above the CMC, much of the SDS covers the surface of NCs and thereby micelles do not form. In all cases, no precipitation, coagulation, or flocculation of the NCs was observed. To study the influence of

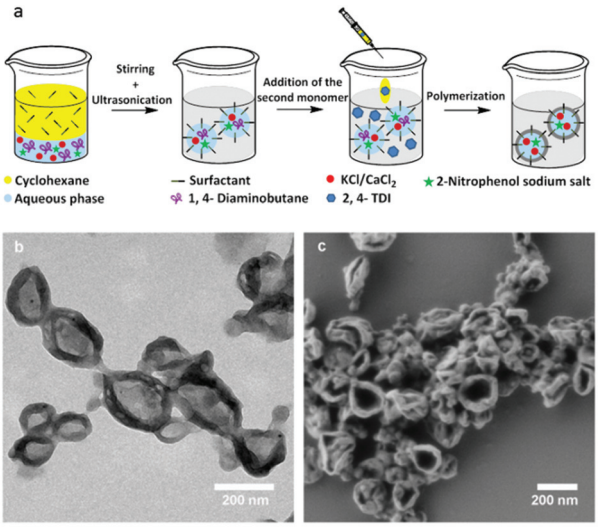

Fig. 1 Schematics for the preparation of the NCs by interfacial polyaddition reaction in inverse miniemulsion (a). TEM (b) and SEM (c) micrographs of the NCs containing 2-nitrophenol sodium salts (sample NPD, Table S1†).

osmotic pressure on the release of payloads from the NCs, the dye 2-nitrophenol sodium salt and different concentrations of salts (KCl or $CaCl_2$) were co-encapsulated. The molar concentration of the dye in the aqueous phase was 0.1 M while the molar concentration of KCl and $CaCl_2$ ranged from 0.1 to 4 M and 0.067 to 2.67 M, respectively. Therefore, the contribution of the dye to osmolarity is very small. 2-Nitrophenol sodium salt (dye) was chosen because it is soluble in water at room temperature and its absorption peak can be clearly detected using UV-spectroscopy. More importantly, it is crucial that the dye does not react with TDI. In general, the reactivity of the group attacking the electrophilic carbon of the NCO group increases as its nucleophilicity increases.[54] This dye does not possess any amino groups and the relative reactivity of the phenolic hydroxyl group of the dye with the NCO group is much lower than that of the primary aliphatic amine ($\sim 10^6$).[54,55] The concentration of $CaCl_2$ was calculated to produce an equal osmolarity to the corresponding KCl concentrations so that the influence of the nature of the salt on the release could be eliminated. It is widely accepted that the thermodynamically-controlled morphology of colloids depends on the interfacial tensions between the continuous and dispersed phases in the presence of a surfactant.[56,57] The TEM and SEM images showed evidence of a core–shell structure for the NCs (see Fig. 1b and c). In the SEM and TEM images, the collapse of NCs is due to the shrinkage of specimens caused by the vacuum chamber of the electron microscopes.

Release of the payloads

A detailed insight concerning the correlation between the releases of the payloads, the dye, and the salts, was obtained by measuring the release of both payloads. The release profile of 2-nitrophenol sodium salt was determined by monitoring

the concentration of the dye with time in the aqueous SDS solution of dialyzed dispersions of NCs. The absorption of the dye could be clearly distinguished and the release could therefore be measured using UV-spectroscopy (see Fig. S1†). The concentration of the salts with time in the release media was measured by ICP-OES (see Fig. S2†). The release profile of the dye depends on the concentration of the co-encapsulated salt (see Fig. 2a). With an increase in the KCl concentration, the fraction of the released dye increased from ~54% (sample NPD) to ~73% (sample NPD[KCl]$_4$) after 24 h. The results also indicate that the release rate in the first hour undoubtedly depends on the KCl concentration. A comparison between the release curves reveals a 92% increase in the release of the dye after 1 h. As expected, the results with the co-encapsulation of $CaCl_2$ instead of KCl exhibited the same propensity as osmotic pressure is a colligative property. This is exemplified for samples NPD[$CaCl_2$]$_{0.067}$, NPD[$CaCl_2$]$_{0.67}$, and NPD[$CaCl_2$]$_{2.67}$ where the concentration of $CaCl_2$ in the dispersed phase is equal to the osmolarity in samples NPD[KCl]$_{0.1}$, NPD[KCl]$_1$, and NPD[KCl]$_4$, respectively (see Fig. S3†). Regardless of the salt types, the molar concentration of the co-encapsulated salt played a controlling role in the dye release. Parallel to monitoring the release profile of the dye, the concentrations of KCl and $CaCl_2$ in the release media were measured. The released fraction of the salts out of NCs with an initial internal osmolarity at t = 1 and 24 h can be observed in Fig. 2b. The release properties of the salts, including the initial release and released fractions, were also dependent on the concentration of salts. The increase in the release rate of salts can be understood by the fact that the salt flux through the NC shell is proportional to the concentration gradient of the salt between the NC core and the release. For example, a ~42% increase in the released fraction of KCl was observed when the KCl concentration in the dispersed aqueous phase was raised from 0.1 M to 4 M. The polyurea shell is permeable to the dye and the salts in the aqueous release medium but to different degrees (see Fig. 2 and S4†). The differences between the release profiles of the dye and KCl with an initial concentration in the dispersed phase of 0.1 M (sample NPD[KCl]$_{0.1}$) emphasize the importance of the payload nature, including its molecular size and possible interaction with the shell of the NCs (see Fig. S4†). The overall and the burst release of KCl are higher than that of the dye. The release rate of KCl is faster than that of the dye because KCl has a lower molecular weight (~78 g mol^{-1}) than the dye (~161 g mol^{-1}).

Measuring the release of the dye and of the salt provided the possibility to determine the correlation type between the release of the dye and the osmotic pressure generated by the salt. The correlation is shown at t = 1 and 24 h (Fig. 2c and d). The results show a non-linear correlation between the released amount of dye and the initial salt concentration in the dispersed phase. This non-linear correlation can be explained by the fact that the dye and the salt have different physicochemical properties, including different molecular sizes. At a salt concentration below 0.25 M, there was hardly any observable increase in the dye release whereas the release was sharply increased at an intermediate salt concentration, *i.e.* between 0.25 and 1 M. Upon a further increase of the concentration of the salt, there was no significant increase of the dye's release on the salt concentration anymore. The maximum release of

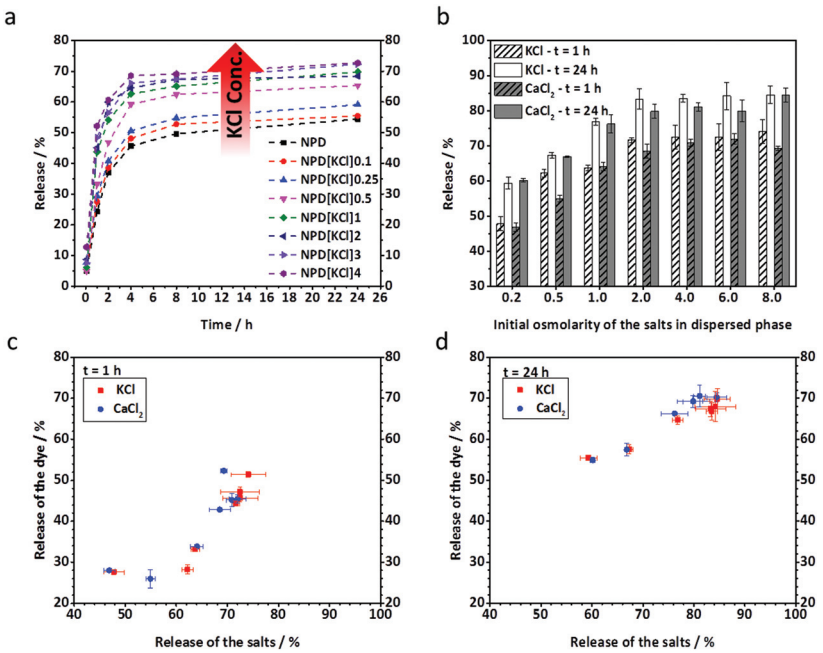

Fig. 2 Temporal release profiles of the dye from NCs consisting of KCl at concentrations between 0 and 4 M in the dispersed phase (a). Release of KCl and $CaCl_2$ from NCs at 1 and 24 h. The salts induced initial osmolarity in the dispersed aqueous phase between 0.2 and 8 Osmol L^{-1} (b). Correlation between the released fraction of the dye and salts at 1 (c) and 24 h (d).

the dye was almost achieved. It can be concluded that a fast release of the dye is triggered with an initial salt concentration in the dispersed phase between 0.25 and 1 M.

Mechanism of release of the payloads

The phenomenon of osmotic pressure has been fully described by Van't Hoff[58] and is defined as pressure differences between the interior and exterior environments of systems separated/enclosed by a membrane. Accordingly, an osmotic substance, *e.g.* water, has the propensity to move through a semi-permeable membrane into the solution containing a solute (*e.g.* salt) until the osmotic pressure differences become equilibrated. This can change the size of the system, causing it to swell. In extreme cases, the disintegration of polymer systems by imposing significant stress on the membrane was reported.[31–33,35,36] The osmotic pressure π_{osm} is related to the concentration of solutes,

$$\pi_{osm} = i\Phi cRT \quad (1)$$

where i is the number of ions produced by solute dissociation, Φ is the osmotic coefficient of the solute, c is the molar concentration of the solute, R is the gas constant, and T is the absolute temperature. The salt concentration can therefore be used to tune a range of π_{osm} and consequently the release profile. The osmotic pressure inside a NC's core varies from ~0.46 to 19.7 MPa (for more details see Table S2†) with an increase in the initial concentration of KCl in the dispersed phase from 0.1 to 4 M. We hypothesized that the co-encapsulation of the salt and subsequently generated osmotic pressure were responsible for the observed differences in the dye release, and the underlying mechanism was the swelling of NCs as shown in Fig. 3a. NCs fabricated with diethylenetriamine were synthesized to obtain NCs with crosslinked shells (Table S1†). Crosslinking is expected to have an effect on the shell rigidity[41] and consequently hinder the release by obstructing the swelling of the NCs despite an osmotic pressure difference. A comparison between the release properties of KCl-loaded NCs with and without crosslinkers showed a decrease of the initial release and of the released fraction of the dye (Fig. 3b). The results showed that the initial burst release generated by the co-encapsulation of salts was largely hindered by crosslinking. To investigate the contribution of the swelling effect to the release profile, DLS measurements were carried out for different NCs after dilution (X = 40) of the aqueous dispersion of these NCs at time intervals t = 0 min and t = 240 min (Fig. 3c). One of the interesting properties of the NCs loaded with KCl is that they deswell (sample NP[KCl]$_1$). The swelling of the NCs caused by the salt osmotic pressure was therefore confirmed by the observed reversible deswelling. The deswelling can be explained by the fact that the shell is permeable towards the co-encapsulated salts. The NC size increases (by ~40 nm in diameter) because of a flux of water into the inner core to reduce the osmotic pressure. The swelling of the shell induced an increase of permeability of the shell for both the dye and salt. When the salt was released, the shell started to deswell and the permeability

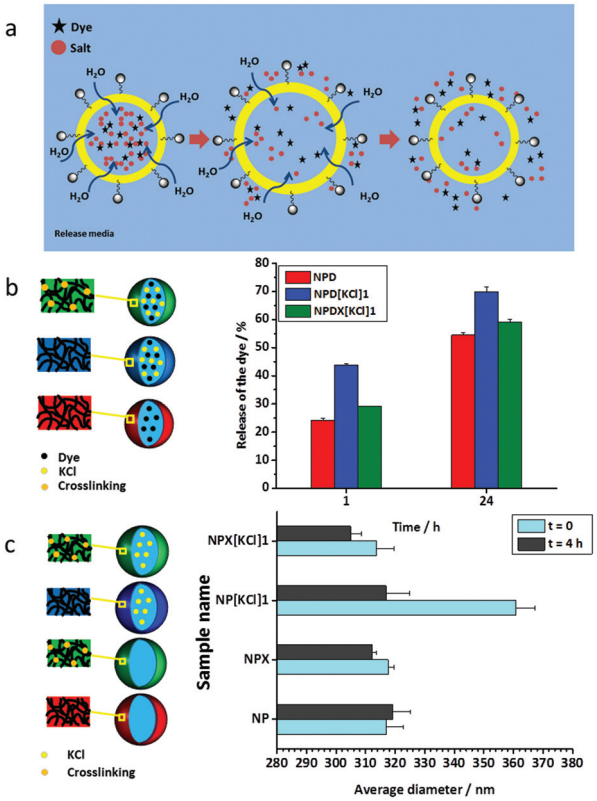

Fig. 3 (a) Schematic illustration of the release of the dye from NCs induced by osmotic pressure. I: The osmotic pressure between the inner core and the release medium is equalized with the flux of water through the shell. II: Swelling of NCs leads to an increase in the dye and the salt release. III: Payload release results in a decrease of the osmotic pressure inside the core and the subsequent deswelling of NCs. (b) Release of the dye from KCl-loaded NCs in the absence (NPD[KCl]$_1$) and the presence (NPDX[KCl]$_1$) of the crosslinker at t = 1 and 24 h. (c) Hydrodynamic average diameters of the non-loaded NCs (NP), non-loaded crosslinked NCs (NPX), NCs loaded with KCl (NPX[KCl]$_1$), and crosslinked NCs loaded with KCl (NPX[KCl]$_1$) at t = 0 and 4 h. The values of these hydrodynamic average diameters were determined by the extrapolation of value for q = 0 (zero angle) (for details please see the ESI and Fig. S6†).

decreased. Afterwards, the salt concentrations both outside and inside the NCs are equalized and the NCs hence start to deswell (see Fig. 3c). The polydispersity indices of sample NP and sample NP[KCl]$_1$ were measured to be ~0.09 and ~0.12 after dilution of the aqueous dispersion of these NCs at t = 240 min, respectively. Because the hydrodynamic average diameters (see Fig. 3c) and polydispersity indices of samples NP and NP[KCl]$_1$ at t = 240 min are not significantly different, it can be concluded that the size distribution of the NCs does not depend on the concentration of the co-encapsulated salt. Therefore, the observed difference in the hydrodynamic diameter size between sample NP and sample NP[KCl]$_1$ after dilution of the aqueous dispersion of these NCs at t = 0 min (~40 nm in diameter) was attributed to the osmotic pressure difference in the core. Moreover, roughly unchanged sizes for sample NPX[KCl]$_1$ (Fig. 3c) explain why the addition of diethylenetriamine in sample NPDX[KCl]$_1$ hinders the increase in the

dye release when the salt is co-encapsulated (Fig. 3b). Diethylenetriamine leads to crosslinking between the polymer chains in the NC shell by providing an additional secondary amine group and therefore hampers the increase of size induced by osmotic pressure. As a consequence, a small increase in the release of the dye was observed for sample NPDX[KCl]$_1$ in comparison with sample NPD[KCl]$_1$ at t = 1 and 24 h.

The presence of ions influences many polymer properties in an aqueous system (*i.e.* lyotropic or Hofmeister effects). According to the typical Hofmeister series, salts may either cause salting-out or salting-in of polymers which largely depends on the type of hydrated anions and hydrophobicity/hydrophilicity of the polymer groups.[59–61] Therefore, it is reasonable to assume that permeability change may happen when the salt concentration changes due to swelling/deswelling of the shell as a result of either salting out or in.[62–64] The polyurea mentioned in this study is rather hydrophobic and, therefore, the polymer shell can be salted out at high concentrations of salts. When salts are released from NCs, the polymer shell may swell and thereby the shell permeability increases. The lyotropic effect of the salt concentration on the release properties is part of the overall change in the NC size measured by DLS. In other words, the NC swelling measured by DLS is the sum of the swelling of the shell and of the core. The effect of the ions on the shell properties increases at higher salt concentrations.

The Young's modulus of the capsule shell can be estimated based on the fact that capsules swell owing to excess osmotic pressure. If the capsule swells from an initial radius (r_0) to a final radius (r), the Young's modulus can be estimated with:[30,65]

$$r \approx r_0\left(1 + \frac{r}{4h}\frac{i\Phi cRT(1-\nu)}{E}\right) \quad (2)$$

where h is the shell thickness, E is the Young's modulus of the polymer and ν is the Poisson ratio. The shell thickness of sample NP[KCl]$_1$ was measured to be 36 ± 13 nm from the TEM image (see Fig. S5†) and r (*i.e.* the radius of swollen capsules) and r_0 (*i.e.* the radius of deswollen capsules) were estimated to be 180 and 158 nm, respectively, by using DLS measurements for sample NPDX[KCl]$_1$ (Fig. 3c). The Poisson ratio of bulk polyurea is 0.49.[66,67] Using eqn (2), the Young's modulus of the polyurea shell was then calculated to be ~18.9 MPa – a value close to the ~27 MPa reported for an aliphatic–aromatic polyurea in bulk.[57] However, when discussing the mechanical properties of the polyurea shells, one has to consider the peculiar stress–strain response of bulk polyurea. For stresses up to about 7 MPa, corresponding to strains of about 10%, polyurea shows a linear elastic response with the above Young's modulus. Beyond that stress value, it behaves much softer with an almost plateau-like stress–strain curve, that allows reaching large strains of several 100% before reaching the failure stress.[57] A change of radius from 158 nm to 180 nm corresponds to a strain of 30%, which implies that in fact a linear elastic regime was already slightly exceeded in that experiment and the use of eqn (2) will underestimate the Young's modulus of the shells for smaller strains. The plane stress σ in the shell of a spherical capsule due to an osmotic pressure difference π across it is given as:[58]

$$\sigma = \pi r/2h \quad (3)$$

where r is the capsule radius and h is the shell thickness. For a shell thickness of 36 ± 13 nm (sample NP[KCl]$_1$ – see Fig. S5†) and a capsule radius of 158 nm, we obtain a stress value of 5.1 MPa for NPD[KCl]$_{0.25}$, which is within the linear elastic regime (<7 MPa), where polyurea reacts relatively stiffly (steep slope in stress–strain curve). For the NPD[KCl]$_{0.5}$ sample the stress reaches 9.9 MPa, which is beyond the linear elastic regime, where the response of polyurea becomes much softer (plateau-like stress–strain curve). This transition in the mechanical response may be responsible for the disproportionate increase in the release observed in Fig. 2a between NPD[KCl]$_{0.25}$ and NPD[KCl]$_{0.5}$. As soon as the stress within the shell exceeds around 7 MPa, small further increases in stress will lead to large strains, which in turn should lead to an increased permeability. This kind of material response of polyurea should have two effects on the release properties: first, by adjusting the size of the particles, one can easily tune the osmotic pressure at which transition between the two regimes and therefore the maximum boost in release occurs. According to eqn (3), a nanocapsule with a mean diameter of 500 nm can resist a 100 times higher osmotic pressure that is needed to rupture microcapsules consisting of the same shell-forming materials with a mean diameter of 50 μm. Second, capsules may be more stable against rupture by osmotic stress than expected from eqn (3) and a given failure stress obtained from a stress–strain curve. For large osmotic pressures, capsule shells will experience large strains, which may lead to a large permeability and possibly to a fast enough reduction in the osmotic pressure before rupture can occur.

Application for biomedicine and anticorrosion

Finally, we illustrated how this approach can be applied to induce either triggered release or sustained release profiles through two different applications, which are the encapsulation of potassium thiocyanate (KSCN) for anticorrosion and foscarnet as a drug for biomedical application (Table S3†). KSCN is harmful for humans by inhalation, in contact with the skin, and if swallowed.[68] Therefore, it is suitable to reduce unnecessary exposure to KSCN *via* encapsulation. KSCN in contact with ferric ions produces a solution, which is red due to the formation of a thiocyanate iron complex. The reaction can therefore be used for monitoring iron oxidation. The burst release of KSCN was therefore triggered by encapsulating a solution of KSCN at a concentration of 1 M (see Fig. 4). When the concentration of KSCN was increased, a larger burst release after 1 h was observed, which was characterized by an increase of release from ~53% to ~84% of the released KSCN compared to the initial amount of KSCN in the dispersions. Moreover, the released KSCN after 24 h for sample NP[KSCN]$_1$ was raised by 38% in comparison with the sample containing KSCN with the initial concentration of 0.1 M (NP[KSCN]$_1$).

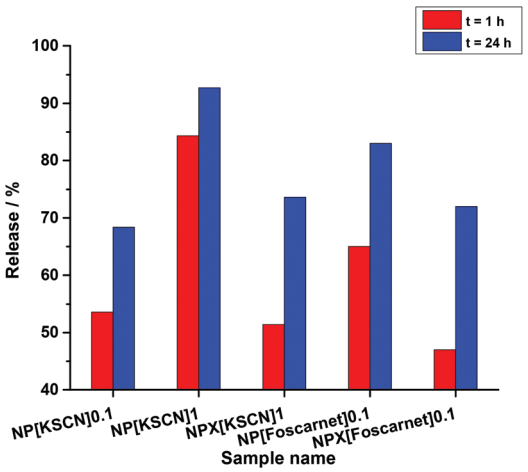

Fig. 4 Released amount of KSCN and foscarnet from NCs. 0.1 and 1 indicate the molar concentration of the payload and X refers to the addition of a crosslinker in the dispersed aqueous phase.

Reducing the burst release is also possible although it is not suitable for sensing applications. Indeed, the addition of a crosslinker reduced the intensity of the initial release generated by osmotic pressure ($NPX[KSCN]_1$). The NCs with KSCN can then be used as optical sensors for the detection of corrosion. Indeed, the color turned from pale yellow-white to red when a solution of ferric ions was added to the dispersion of the nanocontainers (see Fig. S7†). The nanocontainers can be embedded in a protective coating deposited on metals by the electrospinning technique, as was previously reported for other types of nanocontainers containing corrosion inhibitors.[69,70]

The control of the initial burst release generated by osmotic pressure in the core is necessary for many biomedical applications. In fact, drug concentrations *in vivo* can reach near or above the toxic level when the initial release rate is high. Foscarnet, which is an antiviral drug, blocks the pyrophosphate binding site of the viral DNA polymerase at a concentration that does not influence cellular polymerases.[71] However, the poor and variable absorption of foscarnet *via* oral administration, because of a limited capacity or saturation of the phosphate transport system existing in the intestinal brush-border membrane and its decomposition in acidic solution, limits its usage.[72] The encapsulation of foscarnet can overcome the aforementioned limitations if the initial burst release is avoided. Using a crosslinker decreased a part of the initial burst of foscarnet from ~65% to 47%. Additionally, the amount of released foscarnet from the NCs after 24 h for sample $NPX[foscarnet]_{0.1}$ was decreased by ~10% relative to sample $NP[foscarnet]_{0.1}$ as a consequence of the crosslinker addition (Table S3† and Fig. 4). Such a change in the release properties can be considered as a step forward to achieve the release of a drug at a predetermined rate in order to maintain a constant drug concentration for a specific period of time release.

Conclusions

In conclusion, the release of hydrophilic payloads from NCs was controlled by varying the osmotic pressure in the core. To investigate the effect of osmotic pressure on the ratio of the initial burst release to diffusive release, we determined the release profiles for different payloads. The results indicate that the initial release of the payloads from NCs was significantly dependent on the concentration of osmotic pressure agents. The analysis showed a non-linear correlation between the release of the dye and the concentration of the co-encapsulated salts. Further measurements revealed that the responsible mechanism for the observed differences between the release profiles of the dye from the NCs loaded with osmotic pressure generating species (*i.e.* the salts) and non-loaded ones is the swelling of NCs. Note that the concentration of the dye was kept as low as 0.1 M so that its influence on osmotic pressure is not significant. The addition of a small amount of crosslinker showed that it is possible to hamper the initial burst release generated by osmotic pressure. This study shows that different release profiles can be programmed *via* the control of osmotic pressure for various applications such as biomedicine or corrosion protection. Burst release can be turned into an advantage for the acceleration of payload release or one can take advantage of diminishing the burst release by changing the physicochemical properties of NC membranes for decreasing release kinetics. The osmotic pressure-dependent release of payloads from hydrophilic cores without the use of stimulus-responsive units can be potentially applied for self-healing materials and drug-delivery.

Experimental

Materials

2-Nitrophenol sodium salt was purchased from Santa Cruz Biotechnology, Inc. 1,4-Diaminobutane (>98.0) and phosphonoformic acid trisodium salt hexahydrate (foscarnet) (>98.0) were purchased from Alfa Aesar. Potassium chloride (KCl) (≥99.0), calcium chloride ($CaCl_2$) (≥96.0), and potassium thiocyanate (KSCN) (≥99.0) were purchased from Sigma Aldrich. 2,4-Toluene diisocyanate (TDI) and cyclohexane (≥99.9) were purchased from Sigma Aldrich. The surfactant Lubrizol U was supplied from Lubrizol Ltd. The potassium, calcium, and phosphorus standard solutions for ICP-OES were purchased from AppliChem GmbH, Chem-Lab NV, and Fisher Scientific respectively. All chemicals or materials were used without further purification. Distilled water was used through all the experiments if not specifically mentioned.

Preparation of the NCs

Polyurea nanocapsules (NCs) were synthesized *via* interfacial polyaddition reaction using the inverse miniemulsion technique according to the procedure explained previously[49] with slight changes as described in this section. Briefly, aqueous phases consisting of KCl, $CaCl_2$, 1,4-diaminobutane, and

2-nitrophenol sodium (see Table S1†) with a total volume of 1.3 g were prepared. 100 mg of the surfactant Lubrizol U was dissolved in 7.5 g of cyclohexane and mixed with the previously prepared aqueous solution. The obtained emulsion was stirred over 1 h at room temperature and then ultrasonicated for 180 s at 90% amplitude in a pulse regime (20 s sonication, 10 s pause) using a Branson Sonifier W-450-Digital and a 1/2″ tip under ice cooling. A solution consisting of 2.5 g of cyclohexane and 262 mg of TDI was added dropwise to the previously prepared miniemulsion. The reaction proceeded for 24 h at RT under stirring. Afterwards, the nanocapsules were transferred into an aqueous phase using the following procedure: 1 g of the nanocapsule dispersion in cyclohexane was mixed with 5 g of aqueous sodium dodecyl sulfate (SDS) solution (0.3 wt%) under mechanical stirring for 24 h at room temperature. The same synthesis procedure was used for the preparation of NCs with different chemical compositions for the aqueous phases (see Tables S1 and S3†).

Release experiments

The investigations on the release of polyurea NCs were carried out by dialysis. For each sample, dispersions of NCs (5 mL) were placed inside a dialysis bag (MWCO 14 000) and then immersed into 195 mL of an aqueous medium with a pH value of 7.4. After a given time, 5 mL of the solution outside the dialysis bag was taken out followed by the addition of an equal amount of fresh solution to keep the amount constant. The amount of the released 2-nitrophenol sodium salt was measured by UV-Vis spectroscopy. A calibration curve was also drawn by measuring a series of 2-nitrophenol sodium salts with known concentrations. The release of co-encapsulated potassium chloride and calcium chloride out of NCs was also quantified by ICP-OES. By measuring a series of potassium ion solutions, calcium ion solutions, and phosphorus ion solutions with known concentrations, the calibration curves for potassium chloride, calcium chloride, and foscarnet were drawn.

Analytical tools

The prepared NCs were characterized by TEM, SEM, DLS, while UV-Vis and ICP-EOS were used to measure the release of 2-nitrophenol sodium salt, potassium chloride, and calcium chloride (see the ESI†).

References

1 H. F. Lodish, A. Berk, S. L. Zipursky, P. Matsudaira, D. Baltimore and J. Darnell, *Molecular cell biology*, Citeseer, 2000, vol. 4, p. 271.
2 P. J. Kramer and J. S. Boyer, *Water relations of plants and soils*, Academic Press, 1995, p. 71.
3 G. Rapatz, J. J. Sullivan and B. Luyet, *Cryobiology*, 1968, **5**, 18.
4 S. T. Boen, *Medicine*, 1961, **40**, 243.
5 A. Raoult-Wack, *Trends Food Sci. Technol.*, 1994, **5**, 255.
6 C. Klaysom, T. Y. Cath, T. Depuydt and I. F. Vankelecom, *Chem. Soc. Rev.*, 2013, **42**, 6959.
7 D. Lensen, D. M. Vriezema and J. C. M. van Hest, *Macromol. Biosci.*, 2008, **8**, 991.
8 J. N. Huckins, G. K. Manuweera, J. D. Petty, D. Mackay and J. A. Lebo, *Environ. Sci. Technol.*, 1993, **27**, 2489.
9 M. Andersson Trojer, L. Nordstierna, M. Nordin, M. Nyden and K. Holmberg, *Phys. Chem. Chem. Phys.*, 2013, **15**, 17727.
10 C. Mora-Huertas, H. Fessi and A. Elaissari, *Int. J. Pharm.*, 2010, **385**, 113.
11 A. L. Becker, A. P. Johnston and F. Caruso, *Small*, 2010, **6**, 1836.
12 H. Bysell, R. Månsson, P. Hansson and M. Malmsten, *Adv. Drug Delivery Rev.*, 2011, **63**, 1172.
13 T. M. Choi, J.-G. Park, Y.-S. Kim, V. N. Manoharan and S.-H. Kim, *Chem. Mater.*, 2015, **27**, 1014.
14 J. A. Zasadzinski, B. Wong, N. Forbes, G. Braun and G. Wu, *Curr. Opin. Colloid Interface Sci.*, 2011, **16**, 203.
15 A. P. Esser-Kahn, S. A. Odom, N. R. Sottos, S. R. White and J. S. Moore, *Macromolecules*, 2011, **44**, 5539.
16 S. De Koker, R. Hoogenboom and B. G. De Geest, *Chem. Soc. Rev.*, 2012, **41**, 2867.
17 J.-K. Kim, E. Lee, Y.-b. Lim and M. Lee, *Angew .Chem., Int. Ed.*, 2008, **47**, 4662.
18 L.-P. Lv, K. Landfester and D. Crespy, *Chem. Mater.*, 2014, **26**, 3351.
19 R. H. Staff, M. Gallei, M. Mazurowski, M. Rehahn, R. d. Berger, K. Landfester and D. Crespy, *ACS Nano*, 2012, **6**, 9042.
20 M. A. C. Stuart, W. T. S. Huck, J. Genzer, M. Muller, C. Ober, M. Stamm, G. B. Sukhorukov, I. Szleifer, V. V. Tsukruk, M. Urban, F. Winnik, S. Zauscher, I. Luzinov and S. Minko, *Nat. Mater.*, 2010, **9**, 101.
21 Y. Ma, W.-F. Dong, M. A. Hempenius, H. Mohwald and G. Julius Vancso, *Nat. Mater.*, 2006, **5**, 724.
22 L.-P. Lv, Y. Zhao, N. Vilbrandt, M. Gallei, A. Vimalanandan, M. Rohwerder, K. Landfester and D. Crespy, *J. Am. Chem. Soc.*, 2013, **135**, 14198.
23 G. S. Parshuram, Microencapsulation of Liquid Active Agents, in *Functional coatings: by polymer microencapsulation*, ed. S. K. Ghosh, John Wiley & Sons, 2006; p. 153.
24 K. M. Gallagher and O. I. Corrigan, *J. Controlled Release*, 2000, **69**, 261.
25 X. Huang and C. S. Brazel, *J. Controlled Release*, 2001, **73**, 121.
26 C.-Y. Wang, H.-O. Ho, L.-H. Lin, Y.-K. Lin and M.-T. Sheu, *Int. J. Pharm.*, 2005, **297**, 89.
27 Y.-K. Lin and H.-O. Ho, *J. Controlled Release*, 2003, **89**, 57.
28 S. Schmidt, P. A. Fernandes, B. G. De Geest, M. Delcea, A. G. Skirtach, H. Möhwald and A. Fery, *Adv. Funct. Mater.*, 2011, **21**, 1411.
29 S. Suzuki, T. A. Asoh and A. Kikuchi, *J. Biomed. Mater. Res., Part A*, 2013, **101**, 1345.
30 O. I. Vinogradova, O. V. Lebedeva and B.-S. Kim, *Annu. Rev. Mater. Res.*, 2006, **36**, 143.

31 B. G. De Geest, C. Déjugnat, G. B. Sukhorukov, K. Braeckmans, S. C. De Smedt and J. Demeester, *Adv. Mater.*, 2005, **17**, 2357.
32 V. D. Gordon, X. Chen, J. W. Hutchinson, A. R. Bausch, M. Marquez and D. A. Weitz, *J. Am. Chem. Soc.*, 2004, **126**, 14117.
33 H. C. Shum, J.-W. Kim and D. A. Weitz, *J. Am. Chem. Soc.*, 2008, **130**, 9543.
34 J. Takeuchi, A. Ohkubo and H. Yuasa, *Chem. - Asian J.*, 2015, **10**, 586.
35 E. Lorenceau, A. S. Utada, D. R. Link, G. Cristobal, M. Joanicot and D. A. Weitz, *Langmuir*, 2005, **21**, 9183.
36 C. Martino, S.-H. Kim, L. Horsfall, A. Abbaspourrad, S. J. Rosser, J. Cooper and D. A. Weitz, *Angew. Chem., Int. Ed.*, 2012, **51**, 6416.
37 J. Wang, B. M. Wang and S. P. Schwendeman, *J. Controlled Release*, 2002, **82**, 289.
38 J. Wang, B. M. Wang and S. P. Schwendeman, *Biomaterials*, 2004, **25**, 1919.
39 L.-Y. Chu, S.-H. Park, T. Yamaguchi and S.-i. Nakao, *Langmuir*, 2002, **18**, 1856.
40 G. Jiang, B. Thanoo and P. P. DeLuca, *Pharm. Dev. Technol.*, 2002, **7**, 391.
41 B. McFarland and J. A. Pojman, *J. Appl. Polym. Sci.*, 2015, 132.
42 C. Gross-Heitfeld, J. Linders, R. Appel, F. Selbach and C. Mayer, *J. Phys. Chem. B*, 2014, **118**, 4932.
43 P. J. Dowding, R. Atkin, B. Vincent and P. Bouillot, *Langmuir*, 2005, **21**, 5278.
44 S. K. Yadav, K. C. Khilar and A. K. Suresh, *J. Membr. Sci.*, 1997, **125**, 213.
45 D. O. Kuethe, D. C. Augenstein, J. D. Gresser and D. L. Wise, *J. Controlled Release*, 1992, **18**, 159.
46 N. A. Peppas and B. Narasimhan, *J. Controlled Release*, 2014, **190**, 75.
47 T. Zehl, M. Wahab, H.-J. Mogel and P. Schiller, *Langmuir*, 2009, **25**, 7313.
48 S.-H. Kim, T. Y. Lee and S. S. Lee, *Small*, 2014, **10**, 1155.
49 C. M. Roland, J. N. Twigg, Y. Vu and P. H. Mott, *Polymer*, 2007, **48**, 574.
50 A. M. Ibrahim, V. Mahadevan and M. Srinivasan, *Eur. Polym. J.*, 1989, **25**, 427.
51 W. Yin, H. Lu, N. Leventis and D. A. Rubenstein, *Int. J. Polym. Mater.*, 2013, **62**, 109.
52 D. Crespy, M. Stark, C. Hoffmann-Richter, U. Ziener and K. Landfester, *Macromolecules*, 2007, **40**, 3122.
53 E. A. G. Aniansson, S. N. Wall, M. Almgren, H. Hoffmann, I. Kielmann, W. Ulbricht, R. Zana, J. Lang and C. J. Tondre, *Phys. Chem.*, 1976, **80**, 905.
54 S. Ozaki, *Chem. Rev.*, 1972, **72**, 457.
55 E. Delebecq, J.-P. Pascault, B. Boutevin and F. Ganachaud, *Chem. Rev.*, 2013, **113**, 80.
56 S. Torza and S. Mason, *J. Colloid Interface Sci.*, 1970, **33**, 67.
57 B. Vincent, Emulsions, in *Colloid Science: Principles, Methods, and Applications*, ed. T. Cosgrove, Wiley-VCH, 2010, 2nd edn, p. 117.
58 K. S. Pitzer, *J. Phys. Chem.*, 1973, **77**, 268.
59 K. D. Collins and M. W. Washabaugh, *Q. Rev. Biophys.*, 1985, **18**, 323.
60 S. Eichler, O. Ramon, Y. Cohen and S. Mizrahi, *Int. J. Food Sci. Technol.*, 2002, **37**, 245.
61 E. Wachtel and A. Maroudas, *Biochim. Biophys. Acta*, 1998, **1381**, 37.
62 Y. D. Livney, O. Ramon, E. Kesselman, U. Cogan, S. Mizrahi and Y. Cohen, *J. Polym. Sci., B: Polym. Phys.*, 2001, **39**, 2740.
63 W. Kunz, P. Lo Nostro and B. W. Ninham, *Curr. Opin. Colloid Interface Sci.*, 2004, **9**, 1.
64 M. Mori, J. Wang and M. Satoh, *Colloid Polym. Sci.*, 2009, **287**, 123.
65 O. I. Vinogradova, D. Andrienko, V. V. Lulevich, S. Nordschild and G. B. Sukhorukov, *Macromolecules*, 2004, **37**, 1113.
66 A. Jain, G. Youssef and V. Gupta, *J. Adhes. Sci. Technol.*, 2013, **27**, 403.
67 A. Amirkhizi, J. Isaacs, J. McGee and S. Nemat-Nasser, *Philos. Mag.*, 2006, **86**, 5847.
68 D. W. Boening and C. M. Chew, *Water, Air, Soil Pollut.*, 1999, **109**, 67.
69 A. Vimalanandan, L.-P. Lv, T. H. Tran, K. Landfester, D. Crespy and M. Rohwerder, *Adv. Mater.*, 2013, **25**, 6980.
70 T. H. Tran, A. Vimalanandan, G. Genchev, J. Fickert, K. Landfester, D. Crespy and M. Rohwerder, *Adv. Mater.*, 2015, **27**, 3825.
71 A. Bacigalupo, A. Boyd, J. Slipper, J. Curtis and S. Clissold, *Expert Rev. Anti-Infect. Ther.*, 2012, **10**, 1249.
72 H. Bundgaard and N. Mørk, *Int. J. Pharm.*, 1990, **63**, 213.